British Geological Survey

Merging fluxgate and induction coil data collected from Eskdalemuir geophysical observatory to produce low-noise, one-second data

Multi-Hazards and Resilience Programme

Internal Report IR/22/020

BRITISH GEOLOGICAL SURVEY

MULTI-HAZARDS AND RESILIENCE PROGRAMME
INTERNAL REPORT IR/22/020

Merging fluxgate and induction coil data collected from Eskdalemuir geophysical observatory to produce low-noise, one-second data

Guanren Wang, Ciarán D. Beggan and Christopher Turbitt

Keywords

geomagnetism, software, magnetic observatory, induction coil magnetometer, magnetic pulsations, noise filtering, spectrogram, Eskdalemuir, INTERMAGNET, long term stability, noise level.

Front cover

Induction coil magnetometer set up installed at the Eskdalemuir Geophysical Observatory, Scotland.

Bibliographical reference

WANG, G., BEGGAN, C. D., & Turbitt, C. 2022. Merging fluxgate and induction coil data collected from Eskdalemuir geophysical observatory to produce low-noise, one-second data. *British Geological Survey Internal Report*, IR/22/020. 31pp.

Lyell Centre, Edinburgh British Geological Survey 2022

BRITISH GEOLOGICAL SURVEY

The full range of our publications is available from BGS shops at Nottingham, Edinburgh, London and Cardiff (Welsh publications only) see contact details below or shop online at www.geologyshop.com

The London Information Office also maintains a reference collection of BGS publications, including maps, for consultation.

We publish an annual catalogue of our maps and other publications; this catalogue is available online or from any of the BGS shops.

The British Geological Survey carries out the geological survey of Great Britain and Northern Ireland (the latter as an agency service for the government of Northern Ireland), and of the surrounding continental shelf, as well as basic research projects. It also undertakes programmes of technical aid in geology in developing countries.

The British Geological Survey is a component body of UK Research and Innovation.

British Geological Survey offices

Nicker Hill, Keyworth,
Nottingham NG12 5GG
Tel 0115 936 3100

BGS Central Enquiries Desk
Tel 0115 936 3143
email enquiries@bgs.ac.uk

BGS Sales
Tel 0115 936 3241
email sales@bgs.ac.uk

The Lyell Centre, Research Avenue South,
Edinburgh EH14 4AP
Tel 0131 667 1000
email scotsales@bgs.ac.uk

Natural History Museum, Cromwell Road,
London SW7 5BD
Tel 020 7589 4090
Tel 020 7942 5344/45
email bgslondon@bgs.ac.uk

Cardiff University, Main Building, Park Place,
Cardiff CF10 3AT
Tel 029 2167 4280

Maclean Building, Crowmarsh Gifford,
Wallingford OX10 8BB
Tel 01491 838800

Geological Survey of Northern Ireland, Department of Enterprise, Trade & Investment, Dundonald House, Upper Newtownards Road, Ballymiscaw,
Belfast, BT4 3SB
Tel 01232 666595
www.bgs.ac.uk/gsni/

Natural Environment Research Council, Polaris House, North Star Avenue, Swindon SN2 1EU
Tel 01793 411500 Fax 01793 411501
www.nerc.ac.uk

UK Research and Innovation, Polaris House,
Swindon SN2 1FL
Tel 01793 444000
www.ukri.org

Website www.bgs.ac.uk
Shop online at www.geologyshop.com

Foreword

This report details the merging of one-second induction coil and fluxgate magnetometer magnetic field data recorded at Eskdalemuir Geophysical Observatory (ESK) in order to compute "improved" daily, one-second time series.

Eskdalemuir is an INTERMAGNET standard magnetic observatory maintained and operated by the British Geological Survey (BGS) in support of industry and scientific research. In addition to operating a network of nine absolute geomagnetic observatories, BGS publishes data, magnetic indices and data products; and provides advice on the measurement and application of the Earth's magnetic field.

Acknowledgements

The authors would like to thank the Geomagnetism engineering team (Tony Swan, Tim Taylor, Ted Harris and Tom Martyn) for installing, operating and maintaining the induction coil magnetometers as Eskdalemuir Geophysical Observatory. We also wish to thank Ellen Clarke for making the LEMI fluxgate magnetometer available to our use.

We also wish to acknowledge the use of the IndCoils_FGE - A software package for merging Fluxgate and Induction Coil developed by Heinz-Peter Brunke of Helmholtz Centre Potsdam GFZ German Research Centre for Geosciences, Potsdam, Germany (Geosci. Instrum. Method. Data Syst., 6, 487–493, https://gi.copernicus.org/articles/6/487/2017/, 2017)

Contents

FIGURES

Summary

This report describes the use of one-second MFS-07 induction coil and DMI FGE89J fluxgate magnetometer magnetic field data recorded at Eskdalemuir Geophysical Observatory in order to compute an "improved" one-second time series for frequencies higher than specified fluxgate operating band. The DMI instrument is a true one-minute system though it can produce one-second data which are relatively noisy in the 0.2 - 0.5 Hz band. The induction coils are sensitive for periods between 0.1 Hz and 50 Hz allowing their high frequency response to complement the low frequency to DC response of the DMI instrument.

A numerical technique is adapted from published algorithms developed for merging one-second data recorded at Niemegk observatory in Germany. Our goal is to combine the long-term stability of the DMI fluxgate magnetometer with the low-noise of the induction magnetometer to capture the natural magnetic field for frequencies down to 0.5Hz. Magnetic field data with long-term stability in the low frequency end and also providing information at high frequencies are useful in the study of space weather storms.

We have determined the improvement by examining the merged time series, computing the coherence and phase of the one-second merged data with that of the induction coil and fluxgate magnetometer data for the two horizontal components as well as plotting the spectrograms of fluxgate and merged frequencies of interest. We repeated our analysis using data from an instrument capable of meeting the INTERMAGNET one-second definitive data standard, the LEMI-025 fluxgate magnetometer, to compute a separate merged one-second time series as an independent check.

We find that a high coherence exists between the two merged time series (LEMI-025/induction coil and FGE89J/induction coil), without phase difference. Spectrograms of the merged time series reveal micro-pulsations that are otherwise masked by the inherent noise from either fluxgate instruments at the frequency band where Pc1 pulsations occur (0.2-0.5Hz). The Pc1 pulsation in the one-second merged time series from Eskdalemuir observatory is also identified in the equivalent spectrogram of the Niemegk observatory from the same day. This proves that the numerical technique created to capture natural field variations in the 0.2-0.5Hz band can be applied effectively for this UK observatory.

1 Introduction

Fluxgate magnetometers installed at geomagnetic observatories are designed to offer reliable long-term stability from one minute to DC over decades to centuries. When measuring the magnetic field, these fluxgate magnetometers are typically sampled at several seconds to create one-minute values for the present generation of systems. However, conventional fluxgate magnetometer data suffer from noise issues at higher frequencies (e.g. greater than 0.1 Hz or periods of less than 10 seconds), in which the inherent instrument noise level exceeds the ambient magnetic field's natural signal.

This particular behaviour is in contrast to the induction coil magnetometers, which are optimised for capturing signals at the higher frequency spectrum (e.g. 0.1-100 Hz), but provide no long-term stability at low frequencies. An induction coil magnetometer relies on measuring induced currents due to the rate of change of the magnetic flux within the coil, which is directly proportional to the change in the magnetic field with respect to time. This quality makes induction coil magnetometers ideal for measuring short-period magnetic field variations, but inadequate for long periods, usually beyond 10 minutes.

The widely-used FGE fluxgate magnetometer is based on an active technique that works on the principle of passing an alternating current through an excitation coil wrapped around a high permeability, saturable core. The magnetic field generated by the current drives the core into saturation at each half-cycle. The varying magnetic field generated in the core is detected as an induced current in an additional sensor coil. When an external field acts on the core and the core is saturated asymmetrically, even harmonics with amplitudes proportional to the amplitude of the external field are generated in the sensor coil. By using two parallel cores with respective excitation coils wound in opposing senses, the fundamental and any odd harmonics cancel because currents in the excitation coil are in antiphase, improving the instrument sensitivity (Jankowski and Sucksdorff, 1996). A circuit designed to detect even harmonic amplitude is incorporated into a feedback circuit, which drives a current through the sensor coil to cancel out the external field over the core, thus maintaining the core in zero field. This feedback current is therefore linearly proportional to the external field and provides the output of the instrument.

To exploit the benefits of the magnetic field measured at an observatory with both types of instruments available, Brunke *et al.* (2017) present a method of merging induction coil and fluxgate data into a single time series for a given day. Their goal is to overcome the inherent noise produced from their FGE instrument between 30 mHz (~30 seconds) and 0.5 Hz (the instrument's Nyquist frequency) during quiet days. The aim is to meet the INTERMAGNET definitive one-second quality standard of 10pT/√Hz at 0.1 Hz (Turbitt, 2014); thereby satisfying the requirement set for low-noise, high-frequency observatory data. The scientific value of revealing the natural field signals in high-frequency data is illustrated in the study of regular Pc1 magnetic pulsations (0.2 – 5 Hz), for example, which is linked to long-term variations and varying external conditions in the magnetosphere (Guglielmia *et al*., 2005).

The study of Brunke *et al.* (2017) employed the fluxgate and induction coil data from Niemegk observatory (NGK) in Germany for the geographical north (X) and east pointing (Y) magnetic field components. Their results demonstrate how the combined time series data suffer no loss of information or phase distortion by comparing the power spectra of the unprocessed FGE with their merged signal. We attempted to apply the method proposed in Brunke *et al.* (2017) by using one-second data simultaneously recorded using FGE and induction coil instruments installed at Eskdalemuir geophysical observatory (ESK). Both ESK and NGK observatories are positioned in the mid-latitudes and so experience similar geomagnetic variation. The aim of our study is to

repeat their analysis, though we will adapt some of the parameters embedded within the software package from Brunke *et al.* (2017). As an additional check, the merged results are compared with high-resolution fluxgate data recorded by a true-one second LEMI-25 magnetometer, on-site at Eskdalemuir, as an independent check to validate our findings.

2 Magnetometers at Eskdalemuir Geophysical Observatory

The Eskdalemuir geophysical observatory is located in the Scottish borders in an electromagnetically quiet part of the United Kingdom, operated and maintained by the British Geological Survey (BGS). ESK also belongs to INTERMAGNET, a network of geophysical observatories that adhere to common standards including the one-second definitive data standard defined by Turbitt (2014).

(a)

(b)

(c)

Figure 1. **(a)** Example of a DTU FGE fluxgate magnetometer at Eskdalemuir observatory, 35 cm in height **(b)** a LEMI-025 fluxgate magnetometer post-installation, 15 cm in height **(c)** an induction coil magnetometer (white tube) during its installation at ESK in 2012, around 1.2 m in length.

Tri-axial fluxgate magnetometers (Pedersen and Merenyi, 2016) developed by the National Space Institute at the Technical University of Denmark (DTU), model number FGE, have been

collecting data at ESK since 2002 and have proven to have good long-term stability (Figure 1a). To provide long-term stability, the FGE instrument design features compensation coils wrapped around quartz tubes in order to keep the sensor drift to less than a few nT per year. According to manufacture specifications, the temperature coefficient is equal to 0.25 nT/°C or less. Magnetic observatories also demand extremely low baseline drift; to reduce base-line drift down to a few nT a year, a marble cube is suspended in two crossed phosphor-bronze strips in order to compensate for any tilt of the sensor foundation and the marble cube is used to mount the three orthogonal sensors. FGE fluxgate magnetometers are part of the Geomagnetic Data Acquisition System developed by the BGS Geomagnetism Team to measure one-second magnetic field signal (Turbitt, 2002). The FGE sensors at ESK are oriented to register the magnitudes of the horizontal magnetic north and east components and the vertical field component.

Beginning in 2013, a LEMI-025 magnetometer was installed and tested on-site to facilitate observatory operations (Figure 1b). The LEMI-025 magnetometer records magnetic vector data at 1 pT resolution along the three components at one-second cadence. INTERMAGNET (Turbitt, 2014) specifies a data resolution of 1 pT to avoid significant quantisation error being introduced into the measured signal for one-second recorded data. This is below the minimum resolvable signal of the instrument (≤10pT/√Hz_@ 10Hz) as defined by the specification. The LEMI-025 user manual states that instrument noise in the 0.01 – 1 Hz band is < 0.01 nT rms, hence this is equivalent to the instrument sensitivity, or smallest resolvable signal. Swan *et al.* (2016) verified that the noise amplitude spectral density of the LEMI-025 is below 10 pT between 0.1 to 0.5 Hz, which indicates LEMI one-second data noise-level performs within the INTERMAGNET-defined standard. In comparison, Swan *et al.* (2016) measured the noise floor of the DTU FGE89J at 40pT/√Hz at 0.1Hz, while the manufacturer gives a sensitivity specification of 0.1nT.

At higher frequencies than 1Hz, the intensity of the natural field signal is small, especially during geomagnetically quiet periods. However, these signals are expected to be registered by the two induction coil magnetometers installed on the ESK site in June 2012 (Figure 1c), which are oriented orthogonally (X and Y) in the horizontal plane. Note, ESK does not have an induction coil installed in the vertical (Z) direction.

3 Method for Combining Fluxgate and Induction Coil Magnetometer Data

Brunke *et al.* (2017) base their data combination method on the fact that the signal of an induction coil magnetometer is proportional to the time derivative of the magnetic field component along the axis of the coil. By integrating the measurements over one second, the variation of the field in a particular component can be recovered. The short period variation of the induction coil values can be compared to those from the FGE and combined to create a smoother version of the FGE dataset. We give a brief overview before detailing the mathematical implementation.

Taking the geographical north component of the geomagnetic field (X), for any given sample time t_0, we will refer to values recorded by the FGE as $X_{FG}(t_0)$. Values recorded shortly beforehand are $t_0 - T_s N$ and afterward are $t_0 + T_s N$ and are used to produce a single output value, called $B_x(t_0)$, which will be the 'merged' value. T_s is the sampling interval and N is the number of samples chosen so the sample width either side of $B_x(t_0)$ is $T_s N$. The same number of one-second integrated induction coil data (i.e., 2N+1) are also required. Due to the low noise content of the induction coil data, directly integrating and averaging the 2N+1 samples for one second provides a smoother curve of the magnetic field variation in comparison to the one-second fluxgate data, X_{FG}.

Mathematically, if we assume that both sensors are co-aligned along a common direction (e.g., North), values of magnetic field at time t_i, for FGE and induction coil magnetometer $\dot{X}_{IC}$ can be expected to satisfy the equation:

$$B_x(t_0) = X_{FG}(t_i) - \int_{t_o}^{t_i} \dot{X}_{IC}(t)dt \quad (1)$$

Eq.1 is the generic equation underpinning the approach used in Brunke *et al.* (2017). Their method assumes that the induced voltage measured over the induction coil (U_{IC}) can be multiplied by a scale factor, C, linking the measured induced voltages of the induction coil to dX/dt, plus a constant offset (ΔU) in the induced voltages with $\dot{X}_{IC} = C \cdot U_{IC} + \Delta U$. Therefore, Eq.1 can be expressed in the form of Eq.2.

$$X_{FG}(t_i) = \int_{t_o}^{t_i} (C \cdot U_{IC} + \Delta U)dt + B_x(t_0) \quad (2)$$

Each second (1s) must contain 2N+1 measurements in order to compute the value for $B_x(t_0)$. The resulting $B_x(t_0)$ represents the noise-reduced value of the magnetic field at time t_0. This method is applicable separately to the X and Y components (and the vertical Z direction, where applicable). The code steps through each second of the entire day, one second at a time. Note that the first and last N values of the day cannot be computed in this implementation, though it is possible to modify the way these data points are treated. Visually, the approach of Brunke *et al*. (2017) is to fit the smoothed curve of the induction coil data to the measured ('raw') FGE data, and where the two curves overlap, exactly at time t_0, represents the noise reduced, desired value $B_x(t_0)$.

The induction coil signal measured in digital counts per day in our system are integrated and sampled to 1s from 0.01s. Unit is volts per count. We first convert this integrated one-second data to volts by multiplying 3.491 x 10^{-6} V/count in the X channel and 3.475 x 10^{-6} V/count in Y. The integrated induction coil voltage in mV for each channel is then divided by a calibration factor (50.169 mV/nT). To use the integrated induction coil data from ESK, Eq.2 is adapted as Eq.3.

$$X_{FG}(t_i) = C \cdot X(t_i) + \Delta U \cdot t_i + B_x(t_0) \quad (3)$$

$X(t)$ represents the integrated induction coil magnetic signal in nT at time t. $B_x(t_0)$ is the merged value, which shifts the induction coil curve vertically; the offset ΔU adjusts the gradient of the curve and the scale factor C adjusts the amplitude of the curve, corresponding to the magnitude of $X_{FG}(t_i)$.The numerical method of fitting integrated induction coil to fluxgate data for the X-component is presented in Figure 2.

Figure 2 shows the measured DMI FGE data in blue and the induction coil data in green, both units are set to nanoTesla. Panels to the left show that their traces are not fitted. The green curve is computed for the fixed central time t_0 to a time t_i, with i varying from $-i$ to $+i$, applied to the induction coil dataset measured at ESK. Panels on the right is where the green line is fitted to the FGE data after calculating the right values for parameters ΔU, C and $B_x(t_0)$, which are solved for as unknowns. The shape of the fitted curve results from the induction coil measurement, which effectively removes instrument noise contained in the FGE data and is replaced with natural field signals registered by the induction coil. However, a trade-off is made between the number of values used (N) and the ability to capture signals with shorter periods. The final value of $B_x(t_0)$ is at the t = 0 point on panels (b), (d), and (f).

For each t_0 and varying t_i, Eq. (3) produces one equation for each t_i to determine these unknowns. After experimenting with the choice of sample width (T_sN) from 10 to 100s, it was empirically determined that merged data is optimal when T_sN is set between 50s and 80s, giving a total time interval of 101s to 161s, thereby producing enough equations to improve numerical accuracy. This is illustrated in Figure 2d and 2f where the curve produced from the parameter adjusted integrated induction coil curve at a time width of 50s and 80s fit better than at 100s (Figure 2b) because the induction coil magnetometer at ESK appears to suffer from noise leakage in the long period (low frequency). Increasing the number of equations does not improve the accuracy of our merged one-second data. This points to the limit of sensitivity of the induction coil. When 50s≤T_sN≤80s, the choice of the 3-dB bandwidth time-product involved in the Gaussian finite impulse filter response is empirically determined to be 0.004, similar to the default value in the software package. The bandwidth time-product equal the two-sided bandwidth (Hz) multiplied by the sample width (1s). Smaller bandwidth products produce larger pulse widths. The length of the impulse response of the filter is given by $2 \cdot o \cdot T_sN + 1$, where the oversampling factor (o) is set to 1. The number of samples that represents the start of the impulse response to peak of impulse response is set as sample width T_sN. Once the green trace is fitted onto the blue trace, the point of merge between the induction coil and FGE data occurs at t_0.

When both fluxgate and induction coil data series are available at a sample rate of 1Hz, T_s=1, leading to sample width $T_sN = N$. Therefore, a single equation is derived for each sample time t_i. If i varies from $-N$ to $+N$, we can obtain the following conditional system for parameters C, ΔU and $B_x(t_0)$, which produces an overdetermined linear system of equations to solve for three unknowns ($B_x(t_0)$, C, ΔU). Brunke *et al* (2017) introduced a solution to the standard least squared approach, by minimising the sum of the square of residuals r_i, assuming random Gaussian noise.

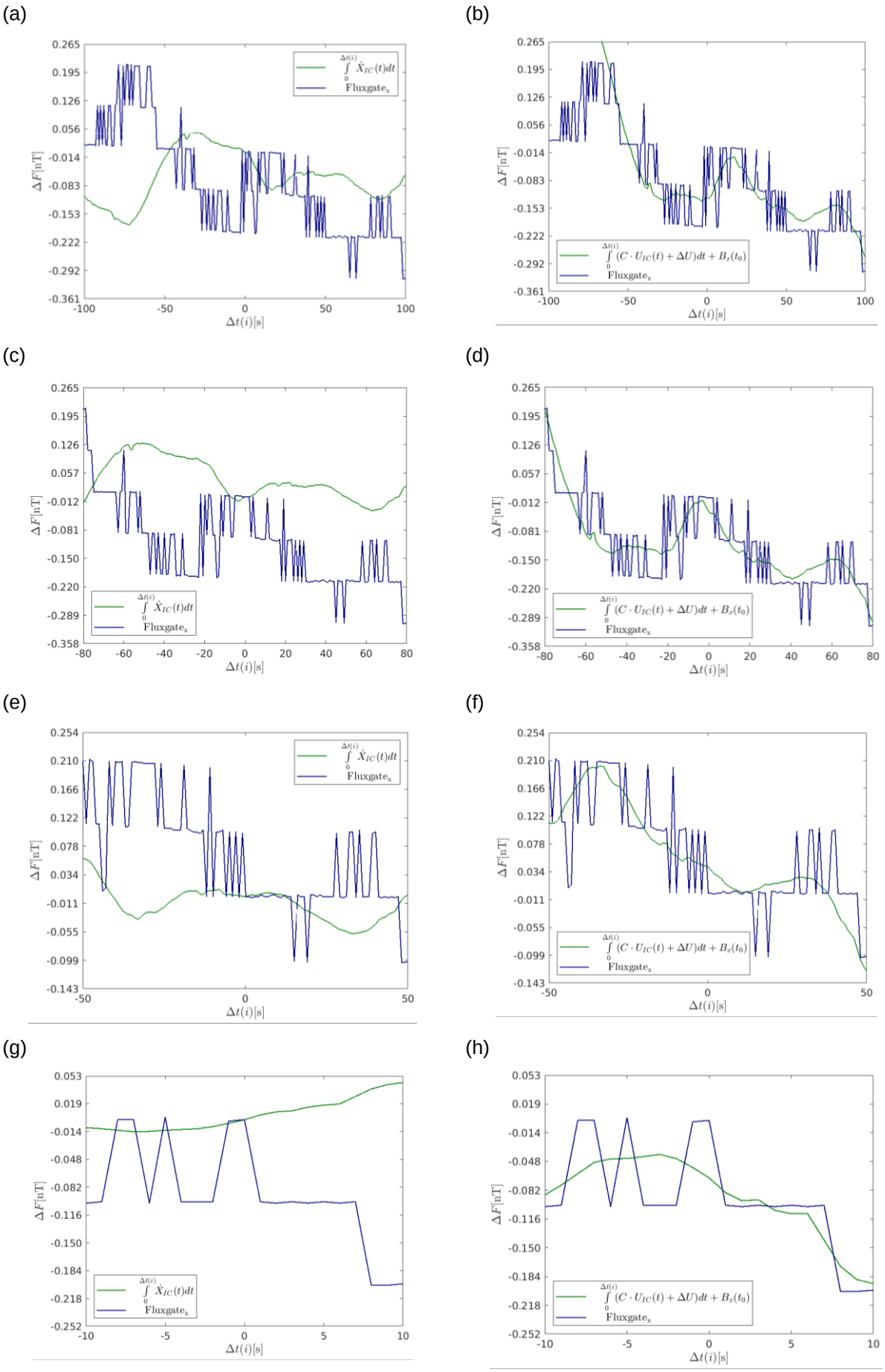

Figure 2. (a) Fluxgate data (blue) with parameters not fitted to the integrated induction coil data (green) both in nT, and N is set to 100s. (b) Green curve fitted to blue curve by adapting parameters C, ΔU and $B_x(t_0)$ in Eq. (2). (c) & (d) N is set to 80s. (e) & (f) N is set to 50s. (g) & (h) N is set to 10s

Setting$S_i = T_s \sum_{k=0}^{i-1} U_{IC}(k)$

produce the following system of linear equations:

$C \cdot S_N + \Delta U \cdot N + B_X(t_0) = X_{FG}(t_N) + r_N$

…

$C \cdot S_i + \Delta U \cdot i + B_X(t_0) = X_{FG}(t_i) + r_i$

...

$C \cdot S_{-N} + \Delta U \cdot (-N) + B_X(t_0) = X_{FG}(t_{-N}) + r_{-N}$

And more explicitly as matrices:

$$\begin{pmatrix} S_N & N & 1 \\ & \vdots & \\ S_i & i & 1 \\ & \vdots & \\ S_{-N} & -N & 1 \end{pmatrix} \cdot \begin{pmatrix} C \\ \Delta U \\ B_X(t_0) \end{pmatrix} = \begin{pmatrix} X_{FG}(t_N) \\ \vdots \\ S_i \\ \vdots \\ S_{-N} \end{pmatrix} \cdot \begin{pmatrix} r_N \\ \vdots \\ r_i \\ \vdots \\ r_{-N} \end{pmatrix} \tag{4}$$

Setting $T_s N$ to 80 s, we get a time interval of 161 s (Figure 2d), and for a sampling rate of 1 Hz, this leads to 161 equations. As long as the number N is much greater than 1, a solution for the unknown parameters C, ΔU and $B_X(t_0)$ exists in the sense of a least squares solution that minimises the sum of the square of the residuals in the form of $Gx = y + r$.To find the set of parameters minimizing the sum of the squared residuals, Eq. (4) is multiplied from the left with the transpose of the matrix on the left-hand side to get the normal equations:

$$\begin{pmatrix} C \\ \Delta U \\ B_X(t_0) \end{pmatrix} = \begin{pmatrix} \sum_{i=-N}^{N} S_i^2 & \sum_{i=-N}^{N} i \cdot S_i & \sum_{i=-N}^{N} S_i \\ \sum_{i=-N}^{N} i \cdot S_i & N(N+1)(2N+1)/3 & 0 \\ \sum_{i=-N}^{N} S_i & 0 & 2N+1 \end{pmatrix} \cdot \begin{pmatrix} \sum_{i=-N}^{N} S_i X_{FG}(t_i) \\ \sum_{i=-N}^{N} i X_{FG}(t_i) \\ \sum_{i=-N}^{N} X_{FG}(t_i) \end{pmatrix} \tag{5}$$

Numerically, this involves solving the 3 x 3 matrix in Eq. 5. This 3 x 3 matrix can solve for the three parameters, including $B_X(t_0)$, which is the improved field signal at time t_0, where six sums are calculated for each sample of the resulting time series. Rather than re-evaluating the sums for each new t_0, the matrix can be updated from the previous step.

In the next section, we show results for merging the one-second data recorded using the two types of magnetometers.

4 Results

4.1 MERGE USING ONE-SECOND FGE FLUXGATE DATA

The FGE and induction coil data for a geomagnetic quiet period recorded at ESK are combined to create the merged time series for X and Y magnetic field components using the method described in section 3.

(a)

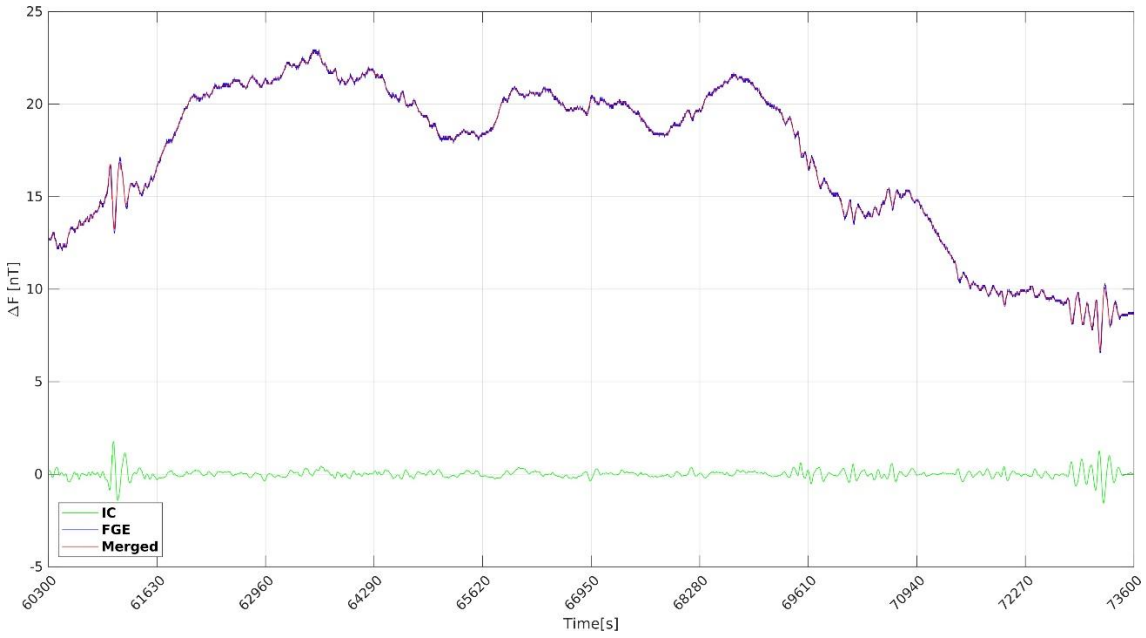

(b)

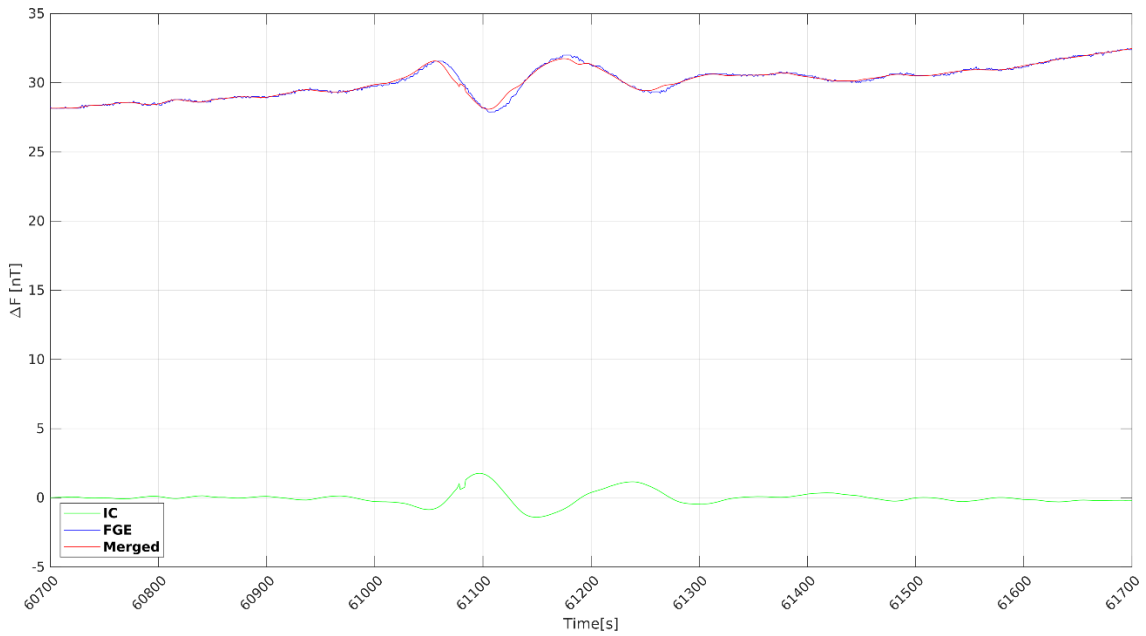

Figure 3**.** (a). Time series of the measured FGE, induction coil (IC) and the merged one-second data for an interval of 60300 to 73600s in the X- component for 05-Jun-2019. All values have a best straight-fit line from the data removed. (b) Zoomed-in between 60700 and 61700s.

The de-trended time series in Figure 3 reveal that the amplitude of variations from the one-second merged data follows the measured FGE fluxgate one-second data closely. The step-like variations in the FGE time series are attributed to the 0.1 nT resolution of the digitiser, which is

sufficient to capture signals above the noise floor of this fluxgate magnetometer. The merged time series is smoother than the fluxgate time series due to averaging. The one-second induction coil time series displays similar variations as the FGE, but are out of phase and contain short-period, low amplitude variations not detected by the fluxgate sensors. For example, Figure 3b shows that the merged data capture the shorter-period signal from the induction coil data around 61080s not observed in the FGE signal.

(a)

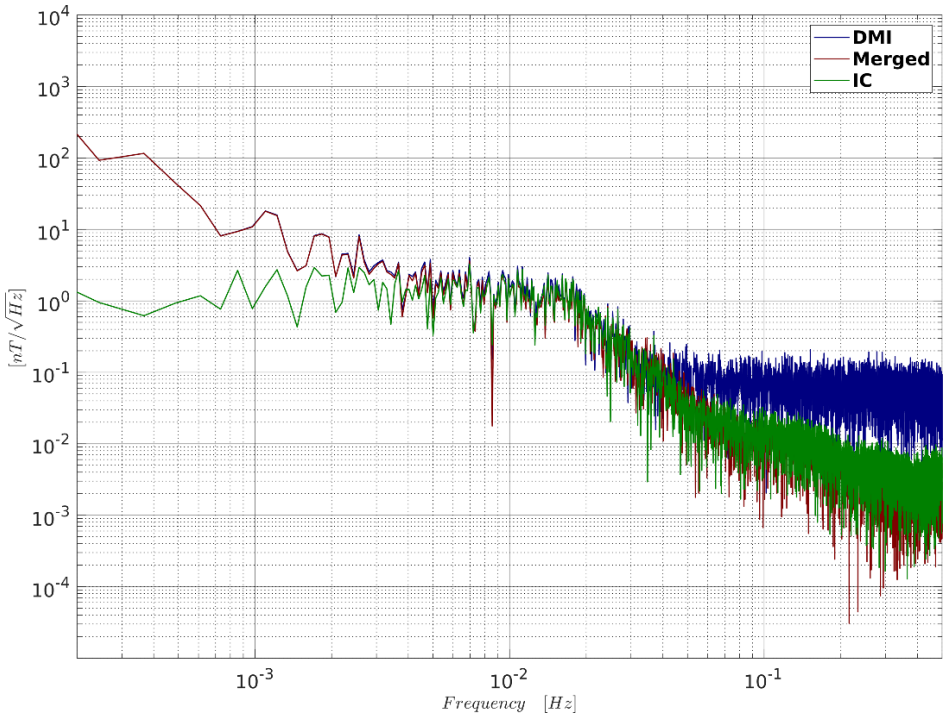

(b)

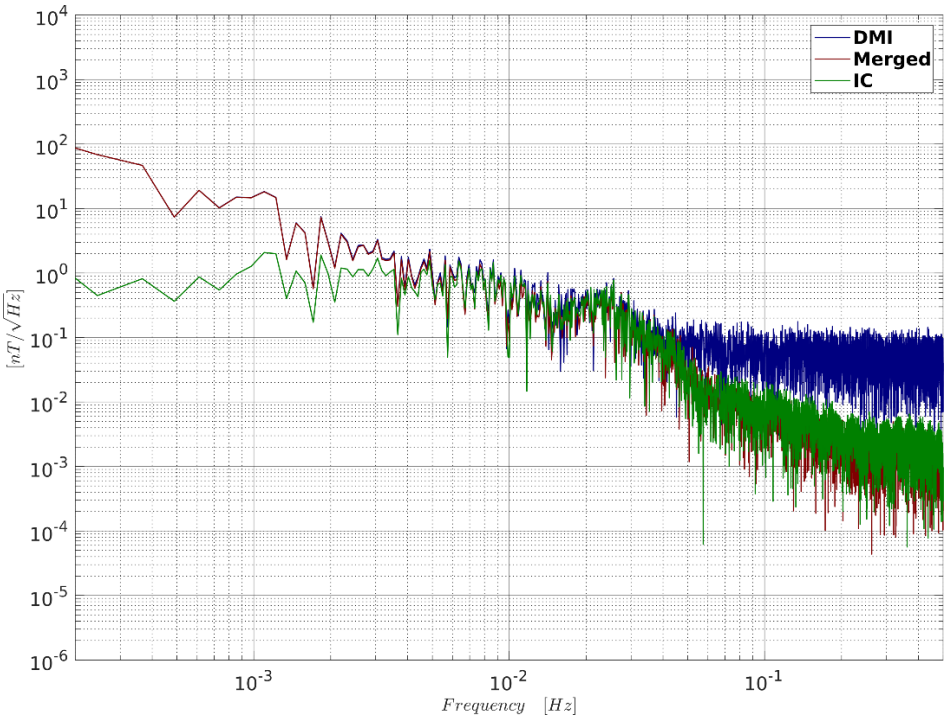

Figure 4. Amplitude spectral densities of the measured FGE (blue), merged (red) and induction coil (green) data, after detrending their input time series, of the entire day for 05-Jun-2019. (a) Shows the X component when sample width is chosen as 50s. (b) shows the Y-component equivalent. The fluxgate-inherent noise floor emerges at frequencies above 40mHz, whereas the induction coil and merged spectra show the continuing decay for the natural field beyond 40mHz as expected.

The improvements in the merged one-second data are demonstrated by comparing linear spectral density from these three one-second data for the same day up to the Nyquist frequency (0.5Hz). The X-component and Y-component linear spectral density in nT/√Hz of the raw FGE and induction coil data in addition to their merged one-second data representative of the natural field for 05-Jun-2019 are shown in Figure 4. The FGE is denoted as DMI (Danish Meteorological Institute) in order to separate it from the LEMI-025 spectra comparison described in section 4.2. All signals are processed using a Discrete Fourier Transform (DFT) of 8192 points sampled at one second, and Hanning filtered to half the NFFT. The DMI FGE fluxgate spectra rolling-off above 40mHz, reaching a constant value close to 40 pT/√Hz at 0.1Hz, in agreement with previous test results of the FGE noise level (Swan *et al.,* 2016). Although the amplitude spectral densities in Figure 4 contain natural signal in addition to instrument noise (as opposed to the measurements conducted by Swan *et al.,* 2016) this .demonstrates that the inherent noise floor of the FGE magnetometer exceeds the INTERMAGNET definitive one-second quality standard of 10 $\mathrm{pT}/\sqrt{Hz}$ at 0.1 Hz (Turbitt, 2014). Above 0.1 Hz, both the merged and induction coil spectra show a continuing decay as expected for the natural field. For frequencies below 10 mHz, the induction coil drifts to 0.9 nT/√Hz whereas the merged spectra follow the FGE spectra very well.

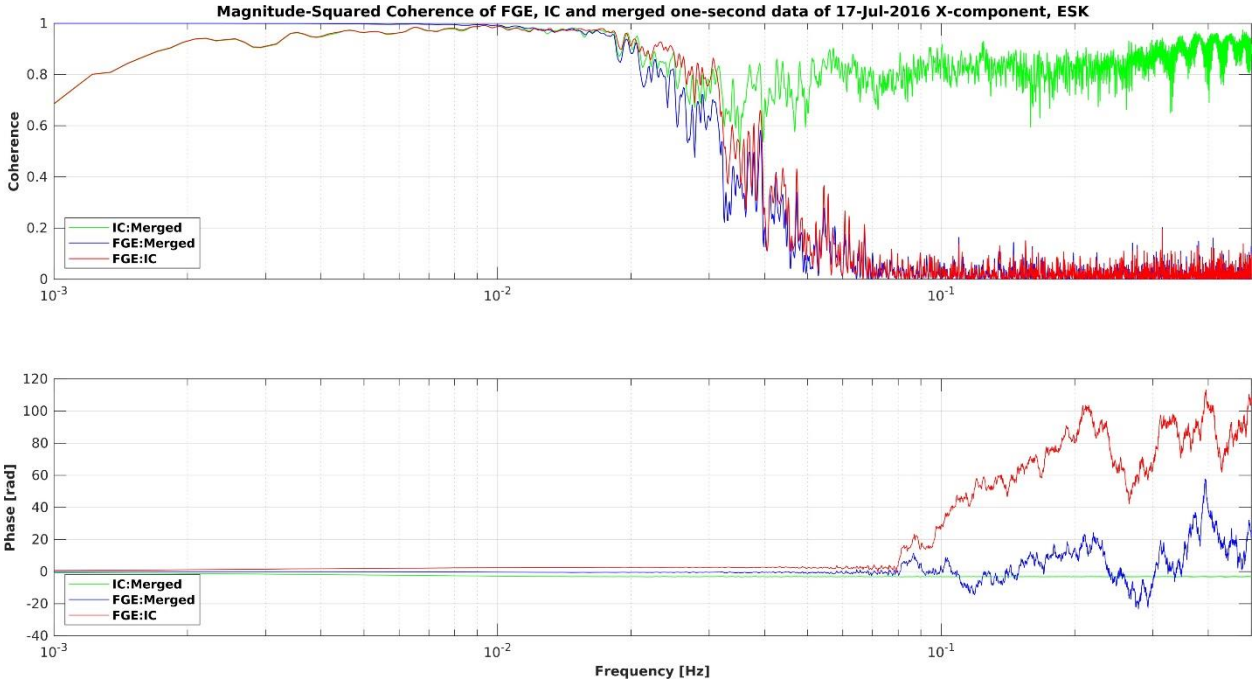

Figure 5. Coherence and phase plot between FGE, merged and IC data for 17-Jul-2016 for the X-component. The sampling width is set to 80s. All signals are set to an NFFT value of 8192. FGE and the merged data show good coherence at low frequencies (<0.01 Hz). The IC and the merged data show good coherence at higher frequencies (>0.01 Hz).

We performed coherency analysis to examine the relationship between the measured one-second IC and FGE signals and the merged data. All values have the linear best-fit removed from the data. The value of the coherence between any two signals, for example between IC and FGE, will satisfy the relationship $0 \leq C_{IC:FGE} \leq 1$, where a magnitude of 1 suggest the two signals are perfectly synchronised at a particular periodicity and 0 denotes a complete absence of synchronisation between two signals. Additionally, the phase difference between two signals are computed to determine if the input signals vary in phase and with the same amplitude as one another. In this instance, we choose to analyse signals for 17-Jul-2016 in the X-component (Figure 5) to compare against the coherence levels reported in Figure 4 of Brunke *et al.* (2017) for the Niemegk observatory; the NFFT is set to 8192 and Hanning filtered to NFFT/2. We can make interpretations based on how well two chosen signals match with one another from looking at their coherence and phase at a particular frequency.

The coherence between the merged and FGE data match well for low frequencies less than 10mHz, but begins to decrease sharply above 30mHz and shows no coherence beyond 40mHz. The IC and the merged time series show minimal phase distortion, but IC/FGE and the merged time series display increasingly larger phase differences at frequencies above 80mHz. Experimentation tells us that only when the sample width, NT_s, is set to 80s and no lower than 50s, do we observe relatively good coherence (>0.5) between merged and IC data at frequencies above the FGE noise level, at approximately 40mHz. This inexact coherence is due to the low energy content of the signal at frequencies between 40mHz and 0.5Hz. Increasing NT_s above 80s does not significantly improve their coherence values between 30mHz and 0.1Hz. The merged and IC coherence reach their maximum coherence value of 0.95 above 20mHz comparable to the inverse value of NT_s selected for the computation of $B_x(t_0)$. Below 10mHz, the coherence decreases because the data have their linear best-fit removed. Hence, it appears that optimal noise reduction is achieved when the sample width is set to 50s to 80s, at least for data measured using instruments at ESK.

Above 0.3Hz, our coherence results for IC and merged one-second data in Figure 5, on a geomagnetically quiet day, is better than that reported in Brunke *et al.* (2017). Interestingly, the coherence reported in Brunke *et al.* (2017) is higher than our results between 40mHz and 80mHz. This could be explained by a combination of better long-period sensitivity of the NGK induction coil magnetometer used in their study compared to those at ESK, but not as well suited for capturing the highest frequency signals as much as the induction coil channels at ESK. The level of coherence between FGE and merged one-second data reported in Brunke *et al.* (2017) is higher than our results for ESK between 20mHz and 40 mHz. This is likely due to the attenuation of the ESK induction coil magnetometer at lower frequencies, which is assumed to be the effect of the integration function of the coils. Whereas the induction coil magnetometer at NGK can capture the natural field at lower frequencies than ESK.

Examples of power spectral spectrograms in $nT^2/\sqrt{Hz}$ are shown in Figure 6 for four selected days at ESK, for which the sample width is set to 80s. Panels on the left provides a visual comparison of the unprocessed DMI fluxgate-only data as spectrograms over 24-hours. The panels on the right show spectrograms produced using the merged data. Panel (a) and (c) show the DMI FGE data on 05-Jun-2019 in the X and Y directions. The geomagnetic activity on the day is low. Spectrograms for the merged data show lower energy overall, after eliminating the instrument noise at higher frequencies, compared to spectrograms generated from FGE-only data. The instrument noise in panel (a) and (c) obscure pockets of energy shown in (b) and (d) even at low frequencies of 30mHz.

Equally important is that spectrograms resulting from the merged one-second data can now better resolve changes up to the Nyquist frequency at 0.5 Hz (i.e. 2 seconds). Panels (e) to (h) show the ambient field response in the X and Y components on 09-Sep-2017 after a major geomagnetic storm caused a Coronal Mass Ejection on 06-Sep-2017. Panel (g) and (h) shows the spectrograms from the FGE-only data and the merged data in the Y component. A Pc1 pulsation appearing at 13:00 to15:00 hours can be identified in panels (g) and (h) between 0.2Hz and 0.4Hz, which corresponds to a period range of 5 to 2.5s. Pc1 pulsations cannot be seen in the fluxgate-only spectrogram. Spectrogram for the Y-component of 03-May-2022 is generated for panels (i) and (j) to compare with Figure 5 of Brunke *et al.* (2017). Panel (j) shows that the Pc1 pulsation observed in the spectrogram of the merged time series computed from combining the induction coil and fluxgate one-second data at Niemegk is also observed in the merged data at ESK. This pulsation occurs at 18:00 UT and is confined between 0.3 and 0.4 Hz. This demonstrates that the numerical technique of Brunke *et al.* (2017) works for ESK data.

In another example, panel (k) reveals a surge in energy on 13-Mar-2022 caused by a geomagnetic storm is obscured by the FGE-noise above 10mHz during 11:00 to 17:00 hrs in the X-component, coinciding with large magnetic intensity fluctuations (black line) during these hours.

Weaker energies are covered by the noise inherent noise floor above 30mHz. Whereas the spectrogram computed using the merged data shown in panel (l) uncovers the energy produced from this storm up to the Nyquist frequency. These examples confirm that the merging method proposed by Brunke *et al.* (2017) also works for geomagnetic storm periods and can reveal micro-pulsations. In the next section, we will compare our merged data with measurements from the LEMI-025 magnetometer over the same period as an independent check.

(a)

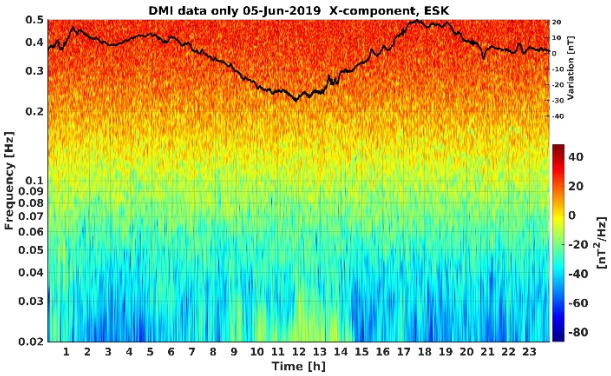
DMI data only 05-Jun-2019 X-component, ESK
Frequency [Hz]
Time [h]
Variation [nT]
[nT²/Hz]

(b)

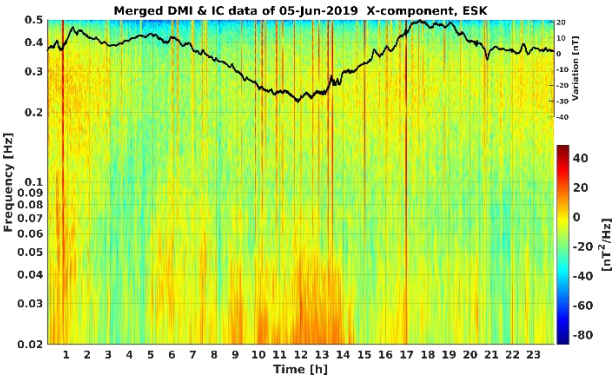
Merged DMI & IC data of 05-Jun-2019 X-component, ESK
Frequency [Hz]
Time [h]
Variation [nT]
[nT²/Hz]

(c)

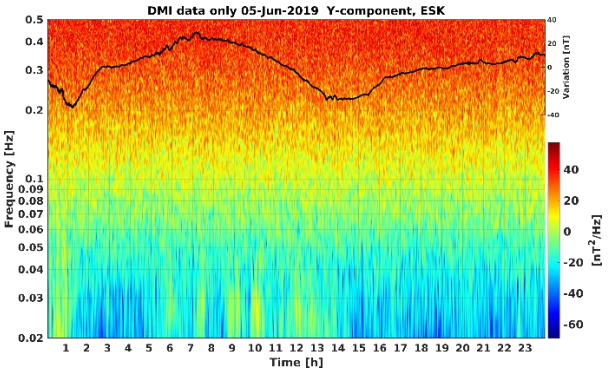
DMI data only 05-Jun-2019 Y-component, ESK
Frequency [Hz]
Time [h]
Variation [nT]
[nT²/Hz]

(d)

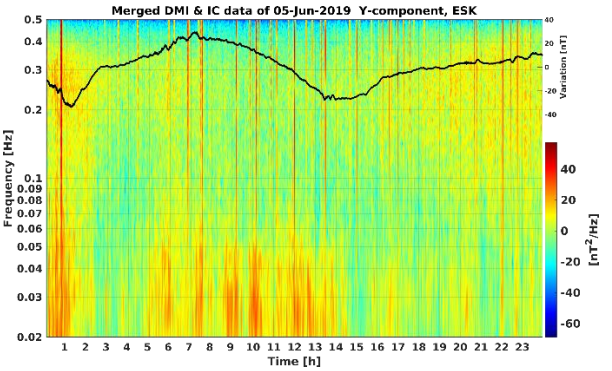
Merged DMI & IC data of 05-Jun-2019 Y-component, ESK
Frequency [Hz]
Time [h]
Variation [nT]
[nT²/Hz]

(e)

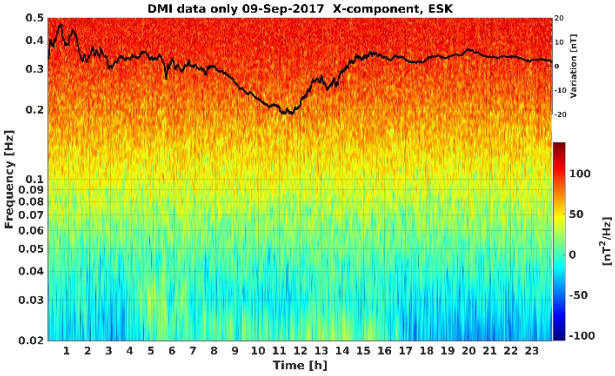
DMI data only 09-Sep-2017 X-component, ESK
Frequency [Hz]
Time [h]
Variation [nT]
[nT²/Hz]

(f)

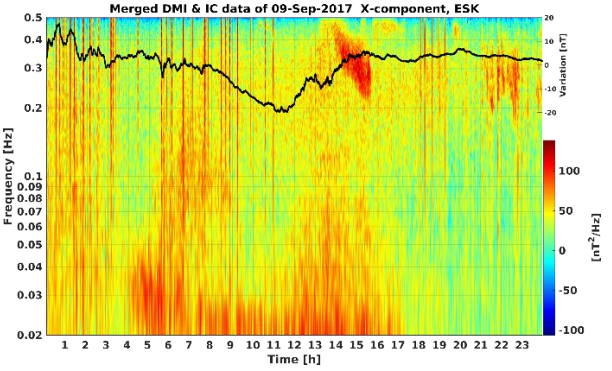
Merged DMI & IC data of 09-Sep-2017 X-component, ESK
Frequency [Hz]
Time [h]
Variation [nT]
[nT²/Hz]

(g)

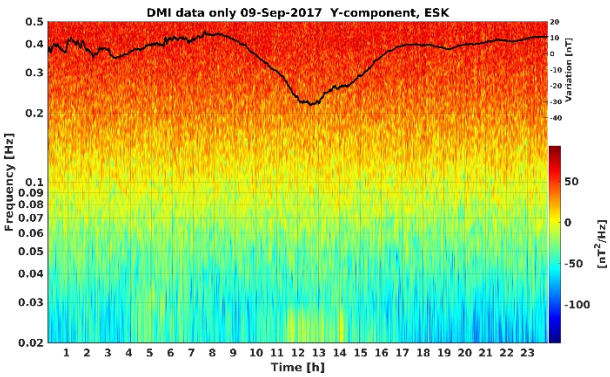
DMI data only 09-Sep-2017 Y-component, ESK
Frequency [Hz]
Time [h]
Variation [nT]
[nT²/Hz]

(h)

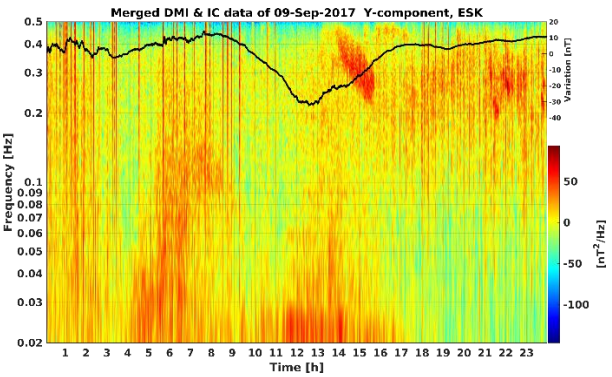
Merged DMI & IC data of 09-Sep-2017 Y-component, ESK
Frequency [Hz]
Time [h]
Variation [nT]
[nT²/Hz]

(i) (j)

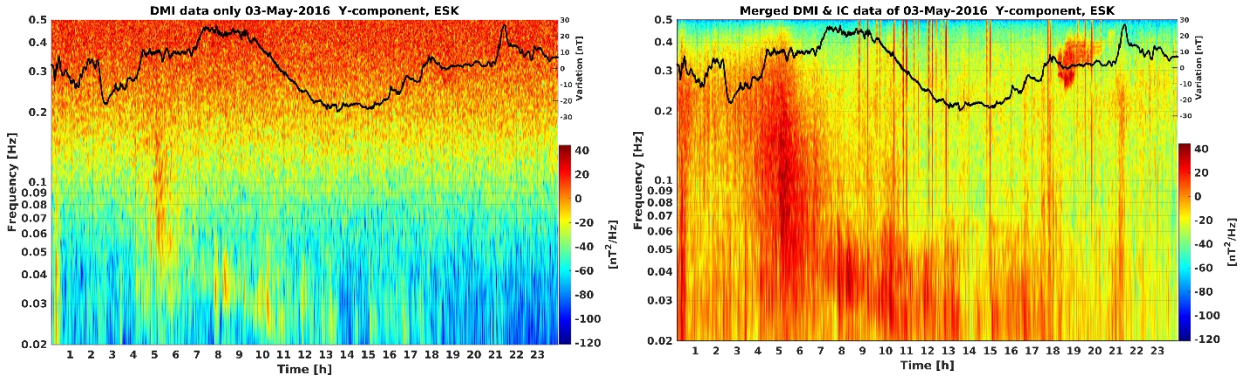

(k) (j)

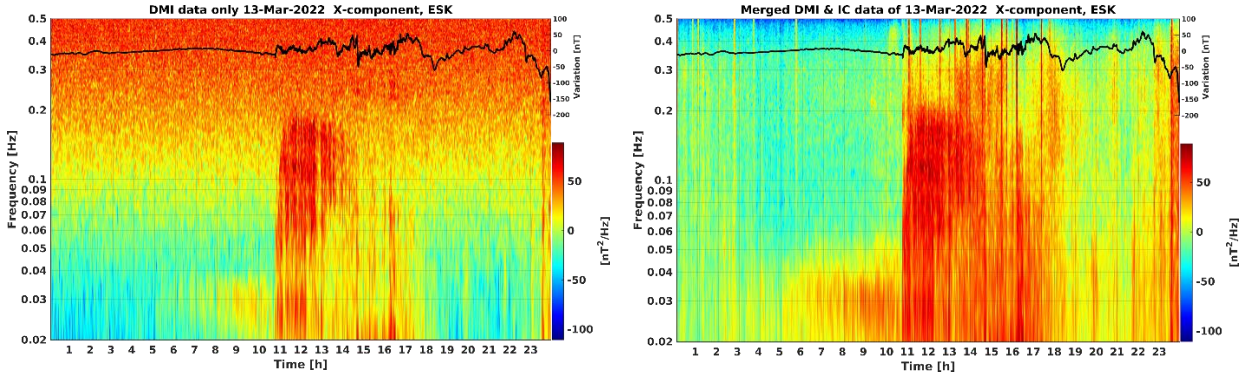

Figure 6. Spectrogram in $nT^2/\sqrt{Hz}$ is overlain with the time series of the natural field in nT (black line). Panels (a) and (b) allow for direct comparison between fluxgate-only and the merged data for 05-Jun-2019 in the X component; Panels (c) and (d) represents the Y component for the same day. Panel (e) to (h) represent Pc1 pulsation observed at 15:00 hrs on 09-Sep-2017 after geomagnetic storm activity for the X and Y components. (i) and (j) a Pc1 pulsation on 03-May-2016 at 18 hrs between 0.3 to 0.4Hz in the Y direction. (k) and (l) shows a large geomagnetic storm that occurred on 13-Mar-2022 in the X component.

4.2 INDEPENDENT COMPARISON USING ONE-SECOND LEMI FLUXGATE DATA

The LEMI-025 magnetometer at ESK observatory was installed on 25-Sep-2013 as a test system. The LEMI magnetometer sensors are expected to register true one-second data because of the instrument noise level is below INTERMAGNET one-second standard. The noise floor estimated by Swan *et al.* (2016) was assessed inside non-magnetic laboratories around ESK, shielded from natural field signals. Since the initial installation of the LEMI-025 magnetometer, the instrument was re-located to separate compartments around the observatory in order to check for discrepancies with the DMI fluxgate data for the horizontal and vertical components during quiet and storm periods. The aim of which is to optimise instrument levelling, temperature, and to test the reliability of data transmission to our geomagnetic data collection system. It is noted that the LEMI data shows less interference (spikes in the time series) than DMI fluxgate data during storm periods. From June 2019, LEMI-025 was modified to measure 10 Hz data in addition to one-second data. One of the observatory objectives is to use LEMI one-second data in place of data recorded by the DMI fluxgate magnetometer sensors once all testing criteria are met, such as to identify any long-term drifts in the data due to instrument tilting. In this section, we begin by looking at the improvements of the LEMI time series, then identify its instrument noise floor before examining the coherence between the one-second LEMI data and the merged one-second data computed using a combination of DMI fluxgate and induction coil data.

(a)

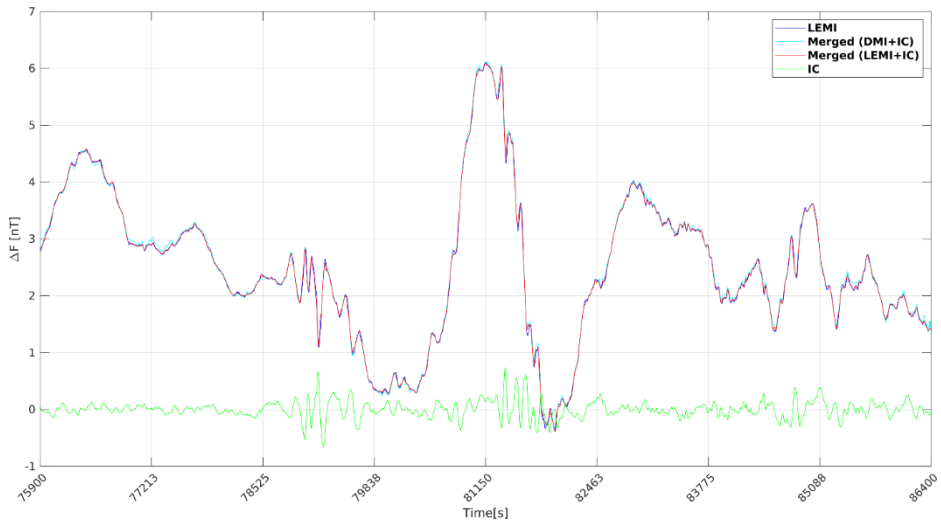

(b)

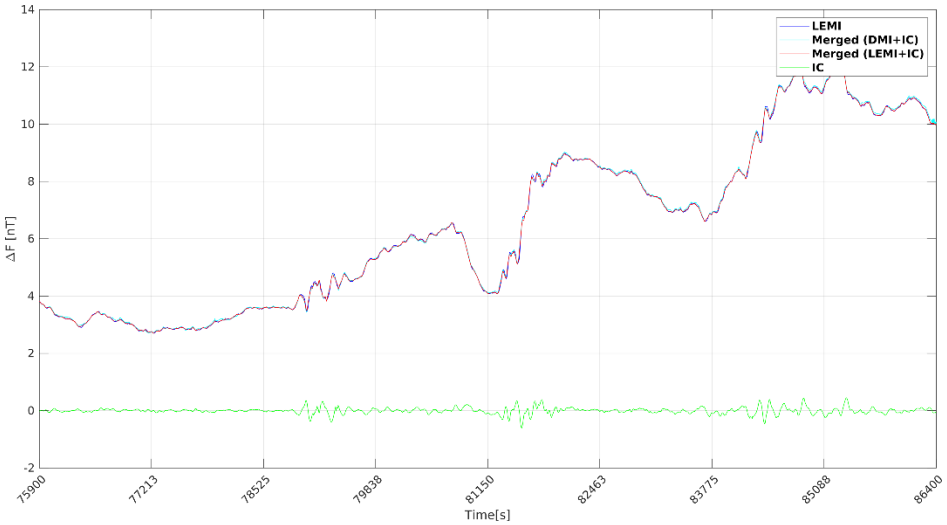

Figure 7. (a) Time series of the measured LEMI one-second data after removing the best straight-fit line from the data, the original merged data from section 4.1, and the second set of merged data computed from combining LEMI and induction coil (IC) data for periods between 76900s and 86400s in the X-component for 05-Jun-2019. (b) Y-component.

The LEMI-025 time series in Figure 7 is smoother compared to the step-like signal variation shown in the DMI fluxgate signal in figure 3 recorded on the same date. This is a result of the 0.1nT threshold of the DMI digitser. The significance of Figure 7 is that the merged time series computed from combining induction coil and the DMI fluxgate magnetometer match closely with the LEMI-only one-second data. As a result, the merged data computed using the LEMI one-second signal (cyan curve) matches well with the merged data using the DMI fluxgate signal (red curve). Subsequent coherence analysis further confirms this. The largest differences between these time series occur during rapid short-period variation; for example, at 77240s, 80780 and 85450s. The one-second induction coil signal is out of phase with LEMI-025 data, especially at periods containing the largest amplitude changes.

(a)

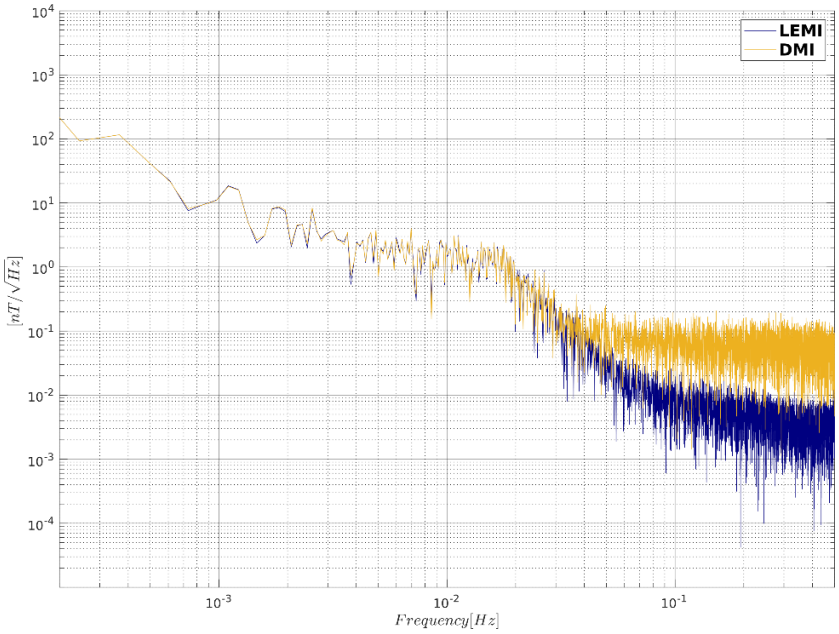

(b)

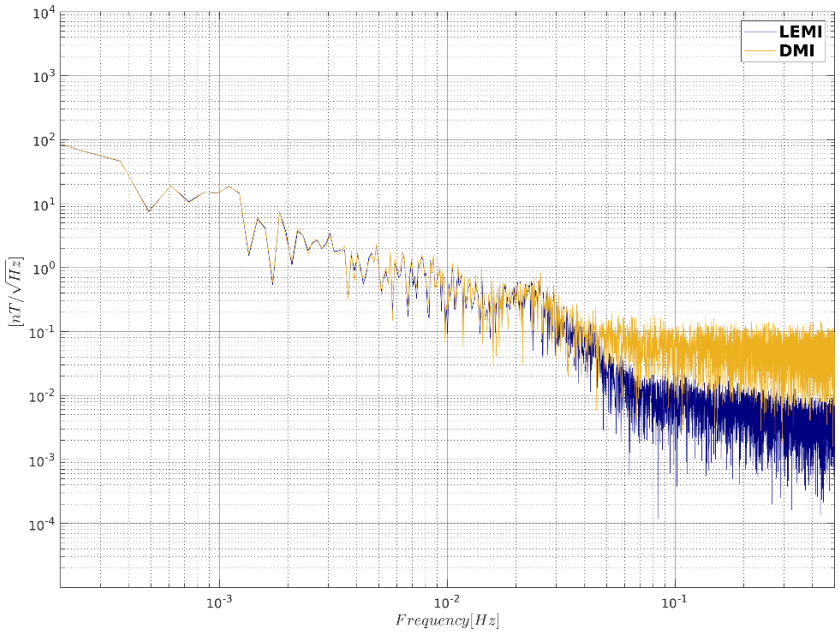

Figure 8. Spectra of measured LEMI (blue) and the DMI fluxgate data (yellow) for 05-Jun-2019. All signals are processed using an NFFT of 8192 points with sampling width both set to 50s. (a) Shows the X component and (b) shows the Y-component.

In

Figure 8, spectra of the measured one-second LEMI-025 data is compared to that of the DMI FGE fluxgate magnetometer data for 05-Jun-2019, a geomagnetically quiet day. The instrument-inherent noise of the LEMI spectra falls to a constant noise level of around 10pT/√Hz frequencies above 0.1Hz. This value is higher than the test results performed by Swan, *et al* (2016) to identify the noise floor of the LEMI instrument due to the inclusion of natural signal in this measurement.

(a)

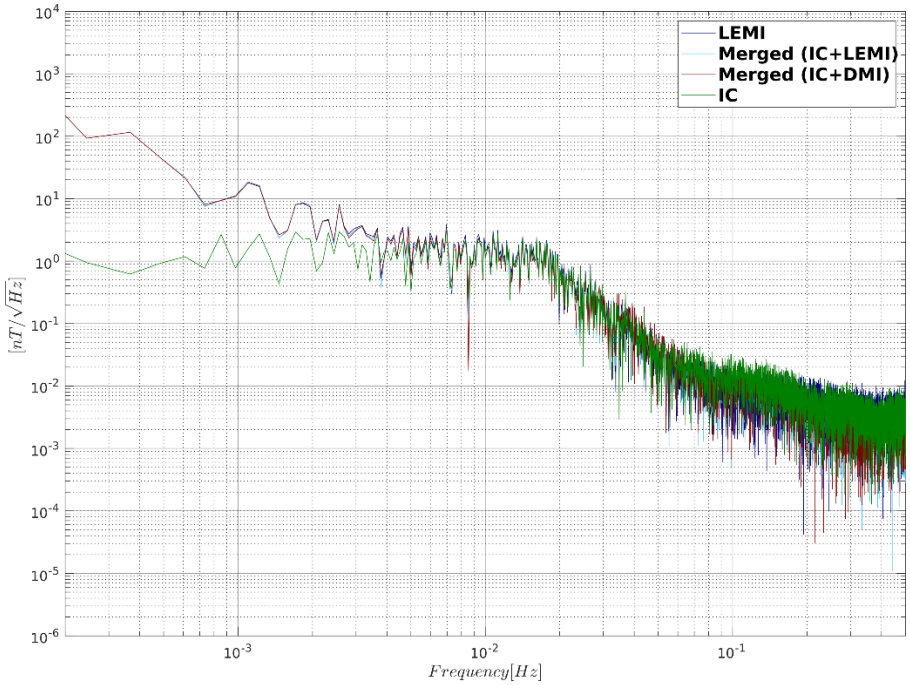

(b)

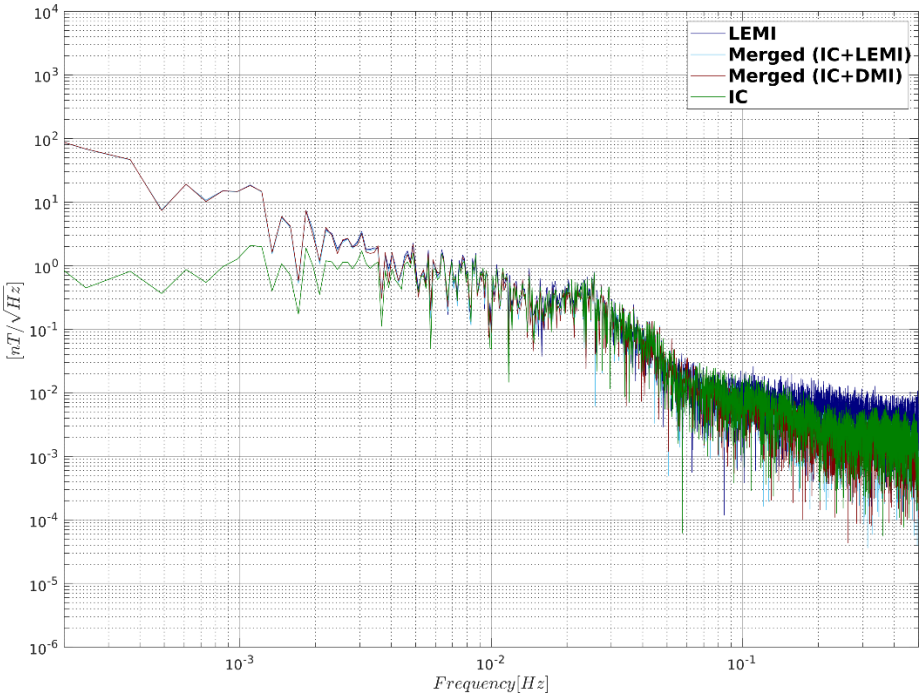

Figure 9. Spectra of measured LEMI (blue), induction coil (IC, red) and the merged data (green) computed from combining LEMI and IC, all detrended for 05-Jun-2019. Sample width set to 50s.All signals are processed using an FFT with length of 8192 points. (a) Shows the X component and (b) shows the Y-component.

Figure 9 shows spectra for the merged data computed using one-second induction coil and the measured LEMI data, with another set of merged data generated by combining induction coil with the DMI fluxgate for the X and Y components. High coherence is achieved in the merged spectra using the LEMI as input compared to the merged spectra using the DMI FGE data as input shown in Figure 4. The constant noise level of the FGE is an order of magnitude higher at 0.1Hz. At frequencies lower than 10mHz, the spectra of LEMI and merged data are identical as expected. Above 10mHz, the two spectra of the merged data both capture the natural decay of the magnetic field up to the Nyquist frequency. A similar signal trace and noise-level is also observed in the Y component. These signal trace and noise-level are observed in both X and Y components.

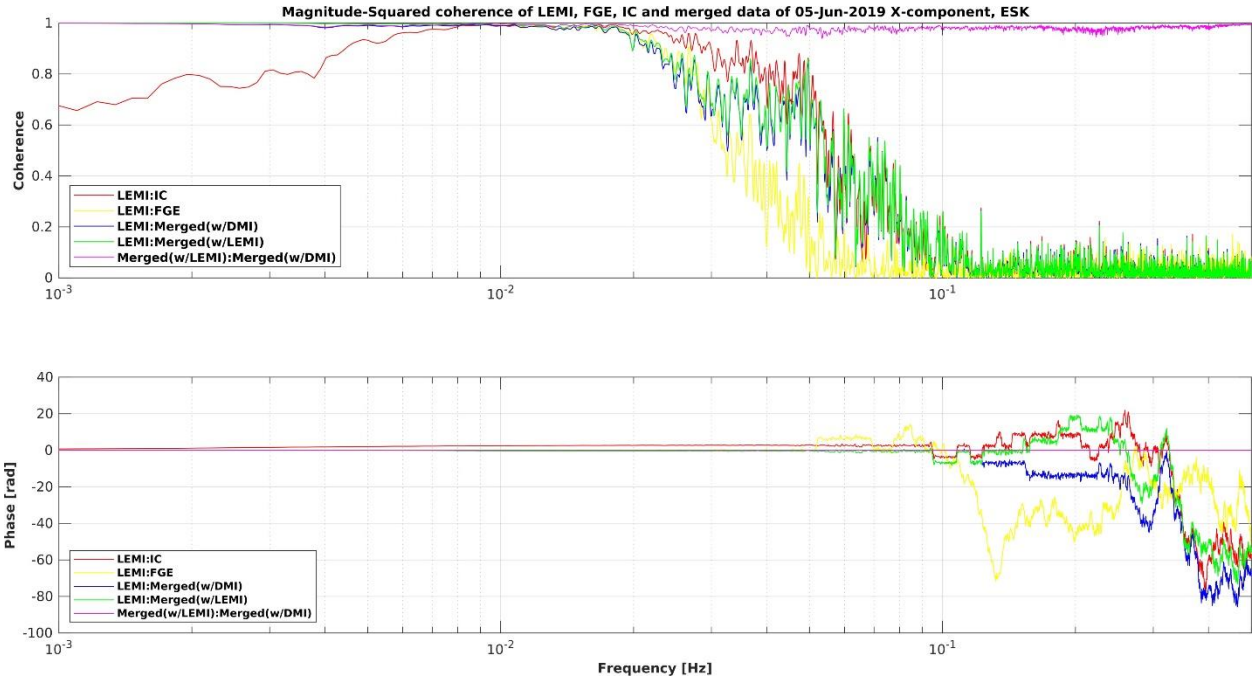

Figure 10. Coherences and phase differences between the measured LEMI, DMI FGE fluxgate, induction coil (IC) recorded on 05-Jun-2019, and the merged one-second data are plotted up to the Nyquist frequency for the X-component.

The merged data computed from combining the induction coil signal with the measured LEMI-025 data, and the merged data computed from combining induction coil signal with the measured DMI FGE fluxgate data show a consistently high coherence and zero phase difference up to the Nyquist frequency (in magenta, Figure 10). The coherence plot also reveals low coherence between the LEMI and the induction coil data (in red) for frequencies above 40mHz, and below 10mHz once the induction coil data drifts.

The coherence and phase differences between LEMI and DMI fluxgate data (in yellow) are poor at higher frequencies where we see a sharp decrease from 0.8 at 25mHz to near zero at 40mHz but increases into high coherence and minimal phase distortion at frequencies < 20mHz. This shows that 1) the LEMI and DMI fluxgate sensors are aligned in the same direction and are calibrated correctly, and 2) the higher sensitivity of the LEMI-025 fluxgate magnetometer at ESK is designed to capture the natural field at higher frequencies, whereas as instrument noise of the DMI FGE magnetometer masks natural field signals at this frequency range. The large phase differences at higher frequencies result from the analogue filter of the DMI FGE data. Furthermore, the high-frequency content of the LEMI-025 data contain mostly noise and are likely to have *leaked* into the merged data below 50mHz, resulting in larger phase differences. LEMI and merged one-second data computed from combining either DMI or LEMI-025 fluxgate data with the induction coil are expressed by the blue and green traces in Figure 10. Both traces show low coherence and large phase differences at high frequencies.

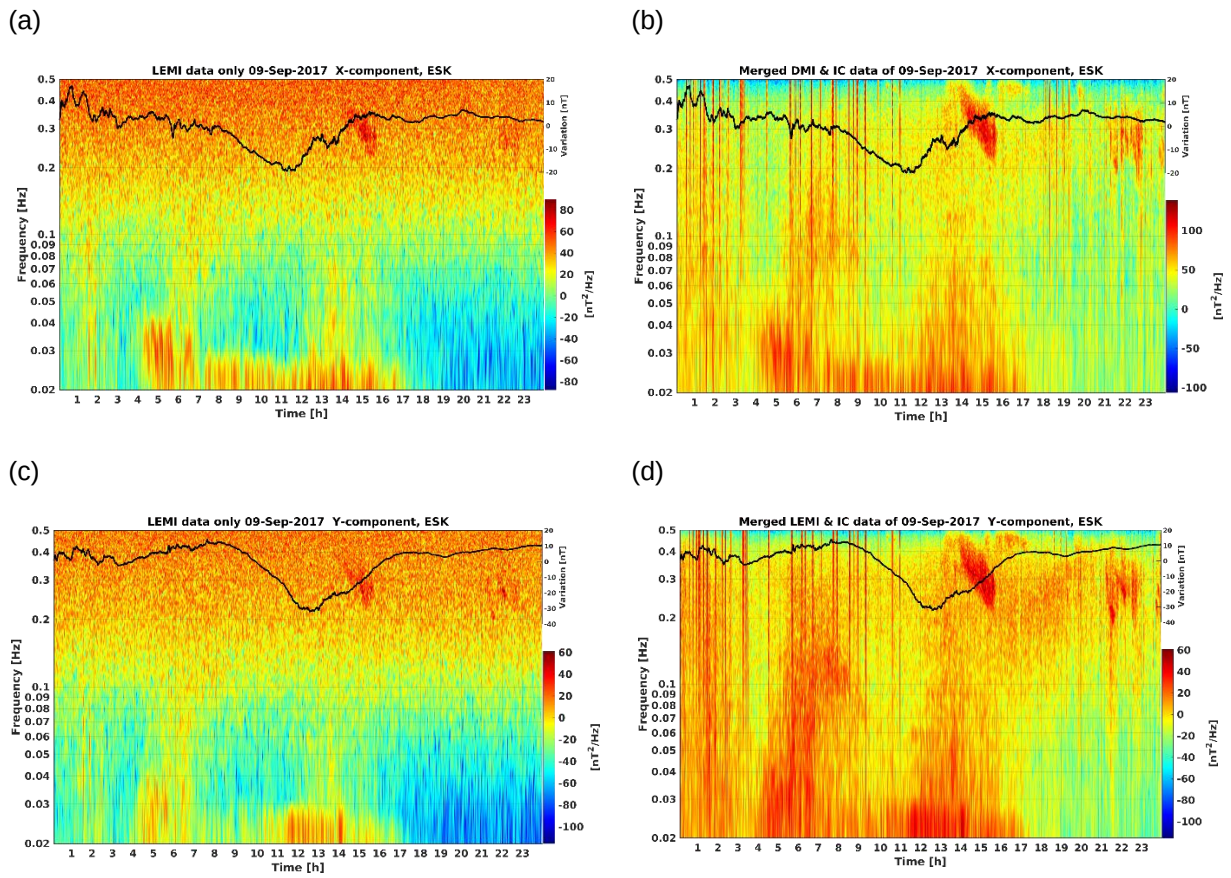

Figure 11. Power density spectrograms ($nT^2/\sqrt{Hz}$) are overlain with the time series of the natural field (black line) for two selected days. Panel (a) and (b) allow for direct comparison between LEMI-only data (a) and the merged data (b) on 09-Sep-2017 in the X component. (c) and (d) represents spectrograms for the for the Y components and the associated merged data.

Power density spectrograms for two selected days used in examples for Figure 6 are displayed in Figure 11. The sample width is set to 80s. Panels (a) to (d) provide a visual comparison of the unprocessed one-second LEMI-025 data and merged data over 24-hours in the X and Y components on 09-Sep-2017, three days after one of the largest geomagnetic storms in the solar cycle. The spectrograms for the merged signal using the measured LEMI-025 data as input show lower energy at higher frequencies overall compared to spectrograms generated from LEMI-only data. The Pc1 pulsation observed in Figure 6f and 6h between 0.3 Hz and 0.4 Hz from merged spectrogram in panels is captured in panels (b) and (d). Unlike spectrograms produced from the DMI FGE-only data (see Figure 6e and 6g), the LEMI-025 spectrogram does not completely mask the higher energy Pc1 pulsation until 0.2Hz, but only obscure it. This is due to a lower noise floor for the LEMI-025 compared to the DMI FGE fluxgate magnetometer, although the weaker ambient field is masked above 30 mHz. Figure 11 shows that the spectrograms generated using LEMI-025 true one-second data as input to produce the merged time series agrees with the spectrograms produced from merged data computed using DMI FGE fluxgate.

5 Conclusion

We applied a least-squares curve fitting technique developed by Brunke *et al.* (2017), which is based on the notion of scaling the integrated induction coil data to fluxgate magnetometer data recorded for in the time domain, in order to compute improved values of the magnetic field in each component for a given period. Our results demonstrate that one-second magnetic field signal recorded by the DMI fluxgate magnetometer and induction coil installed at Eskdalemuir geophysical observatory can be merged into a single time series for the vector components, X and Y.

The power spectral density of the merged signal reveals the natural magnetic field variation during periods of low geomagnetic activity up to the Nyquist frequency of 0.5Hz. Signals recorded by the DMI fluxgate magnetometer for this frequency range would otherwise be masked by the instrument noise. As an independent check, we compared this same merged signal with the one-second LEMI fluxgate data, which already satisfy the INTERMAGNET specification for the minimum resolvable signal at 10pT/√Hz at 0.1Hz.

Results from our analysis of the linear spectral density and the signal coherence confirm a significant improvement to the merged one-second data up to the Nyquist frequency as compared to using either the induction coil or the FGE fluxgate data themselves. The spectrogram produced from the merged one-second data reveal features of the natural field after geomagnetic sub-storm events, such as Pc1 pulsations, that would have not been distinguished from the fluxgate instrument noise. Therefore, it is useful to combine the two measured datasets according to the method established by Brunke *et al.* (2017) at ESK to improve the one-second values generated by the DMI FGE instrument.

Appendix: Code and Data Availability

The MATLAB source code for merging Fluxgate and Induction Coil data can be found at: Brunke, Heinz-Peter; Widmer-Schidrig, Rudolf; Korte, Monika (2017): IndCoils_FGE - A software package for merging Fluxgate and Induction Coil data. V. 1.0. GFZ Data Services. http://doi.org/10.5880/GFZ.2.3.2017.002

Glossary

Fluxgate Magnetometer A zero-field instrument that registers magnetic measurements along a built-in direction. Fluxgate magnetometer is suitable for measuring long-period magnetic field variations. It is sensitive to temperature variations so the coils wrap around thermally stable materials. The FGE installed at Eskdalemuir has three orthogonal sensor units.

Induction Coil Magnetometer A coil of copper wire wrapped around a long, highly permeable core encased inside a shock absorbent casing. The sensitivity of the instrument is highest for high frequency (short-period) fields, including the dead band of magnetotellurics spanning between 30.0 mHz and 0.5 Hz (33.3 s and 2.0 s period).

Geomagnetic Storm Sporadic, short-lived disturbances to the magnetopause due to sudden expulsions of plasma from the Sun's surface. Severe Geomagnetic storms may exert potential impacts to man-made technologies.

References

Brunke, H. P., Widmer-Schnidrig, R., and Korte, M. (2017). Merging Fluxgate and Induction Coil Datato produce low Noise geomagnetic Observatory Data meeting the INTERMAGNET Definitive One-second Data Standard, Geosci. *Instrum. Method. Data Syst. Discuss.,* https://doi.org/10.5194/gi-6-1-2017

Guglielmi, A., Potapov, A., Matveyeva, E., Polyushkina, T., Kangas, J. (2006). Temporal and spatial characteristics of Pc1 geomagnetic pulsations, *Adv. Space Res*, 38, pp. 1572–1575., https://doi.org/10.1016/j.asr.2005.05.027

Jankowski, J. and C. Sucksdorff. (1996) 'Magnetometers' in *Guide for Magnetic Measurements and Observatory Practice*. 1st ed. Boulder: J.A. Jocelyn, International Association of Geomagnetism and Aeronomy, pp. 79-81

Pedersen, L. W. and Merenyi, L., (2016). The FGE Magnetometer and the INTERMAGNET 1 Second Standard, *J. Ind. Geophys. Union*, pp. 30–36

Swan, T., Shanahan, T., Turbitt, C., Rasson, J. (2016). Hardware Developments to Determine the Transfer Function of a 1-Second Fluxgate Magnetometer, *J. Ind. Geophys. Union*, 2, pp. 24-29

Turbitt, C. (2002). Geomagnetic Data Acquisition System – GDAS, https://geomag.bgs.ac.uk/documents/gdas2002complete.pdf

Turbitt, C. (2014). INTERMAGNET Definitive One-Second Data Standard, INTERMAGNET Technical Note, http://www.intermagnet.org/publications/im_tn_06_v1_0.pdf